

Article

Study on Flowability Enhancement and Performance Testing of Ultrafine Dry Powder Fire Extinguishing Agents Based on Application Requirements

Guangbin Lu, Junchao Zhao *, Yanting Zhou, Yangyang Fu, Song Lu  and Heping Zhang

State Key Laboratory of Fire Science, University of Science and Technology of China, Hefei 230026, China; gblu@mail.ustc.edu.cn (G.L.); zhouyanting@mail.ustc.edu.cn (Y.Z.); yyfu@ustc.edu.cn (Y.F.); lusong@ustc.edu.cn (S.L.); zhanghp@ustc.edu.cn (H.Z.)

* Correspondence: zhaojc01@ustc.edu.cn

Abstract: Flowability greatly affects the application of ultrafine dry powder fire extinguishing systems, while hydrophobicity and acute inhalation toxicity are concerns for fire extinguishing agents. In the present study, we examined the impact of hydrophobic fumed silica on the hydrophobicity and flow properties of ammonium dihydrogen phosphate as the base. Our findings revealed that incorporating 6 wt.% of hydrophobic fumed silica resulted in optimal flowability, accompanied by a hydrophobicity angle of 126.48°. The excessive inclusion of hydrophobic fumed silica impeded powder flow within the ammonium dihydrogen phosphate particles. Furthermore, the investigations indicated that the incorporation of a small quantity of bentonite (0.5 wt.%) amongst the three functional additives—bentonite, magnesium stearate, and perlite—offered further enhancements in powder flowability. In fire extinguishing experiments' total flooding conditions (1 m³), the designed UDPA exhibited a minimum required extinguishing concentration of merely 41.5 g/m³, which is better than the publicly reported value. Moreover, observations on the well-being of mice subjected to nearly three times the extinguishing concentration at 60 s, 10 min, and 3 days, respectively, demonstrated the absence of acute inhalation toxicity associated with the designed UDPA. Collectively, the developed ultrafine dry powder fire extinguishing agent displayed promising performance and possesses broad applicability.

Keywords: ultrafine dry powder fire extinguishing agents; hydrophobicity; flowability; Carr flow index; acute inhalation toxicity



Citation: Lu, G.; Zhao, J.; Zhou, Y.; Fu, Y.; Lu, S.; Zhang, H. Study on Flowability Enhancement and Performance Testing of Ultrafine Dry Powder Fire Extinguishing Agents Based on Application Requirements. *Fire* **2024**, *7*, 146. <https://doi.org/10.3390/fire7040146>

Academic Editor: Jinlong Zhao

Received: 6 March 2024

Revised: 6 April 2024

Accepted: 10 April 2024

Published: 18 April 2024



Copyright: © 2024 by the authors. Licensee MDPI, Basel, Switzerland. This article is an open access article distributed under the terms and conditions of the Creative Commons Attribution (CC BY) license (<https://creativecommons.org/licenses/by/4.0/>).

1. Introduction

CF₃Br (Halon 1301), commonly used in fire extinguishing, was restricted due to its high ozone depletion potential [1,2]. The search for alternatives promoted the examination of the effectiveness of several gases, liquids, and dry powder agents. Among them, it was proven that the dry powder agent was the most common and effective among the fire extinguishing agents, which have been widely used and proven to be several times more effective than Halon 1301 [3–6]. As the dry powder agent becomes finer, the specific surface area of the powder increases. This increase in the surface area leads to higher heat absorption and higher fire extinguishing efficiency. Ewing [7,8] found that there is a critical particle size for different powder agents, where the agents can be completely decomposed before it reaches the fire zone. When the particle size of the powder is below this value, the extinguishing performance of the powder will be significantly improved. China's standard defines an ultrafine dry powder extinguishing agent (UDPA) as a particle size less than 20 microns, corresponding to D₉₀ (90% cumulative distribution particle size) [2,9,10].

The UDPA is currently utilized in a variety of applications, including integrated underground tube corridors [11,12], wind turbine enclosures [13,14], and high-rise structures [15,16]. It has been observed that the moisture absorption and aggregation

of particles have a significant impact on the diverse characteristics of the UDPA during storage and usage, serving as pivotal contributors to its failure [17,18]. Particle aggregation occurs during the preparation, processing, and utilization of ultrafine dry powder fire extinguishing agents, particularly when ammonium dihydrogen phosphate (ADP) is used as the primary material. Shown in Figure 1, ADP possesses strong hygroscopic properties and when coupled with a reduced particle size, tends to readily induce aggregation [19,20]. Hence, the primary objective in the development of ultrafine dry powder fire extinguishing agents is to impart hydrophobic properties to the particles, thus addressing the issue of particle aggregation.

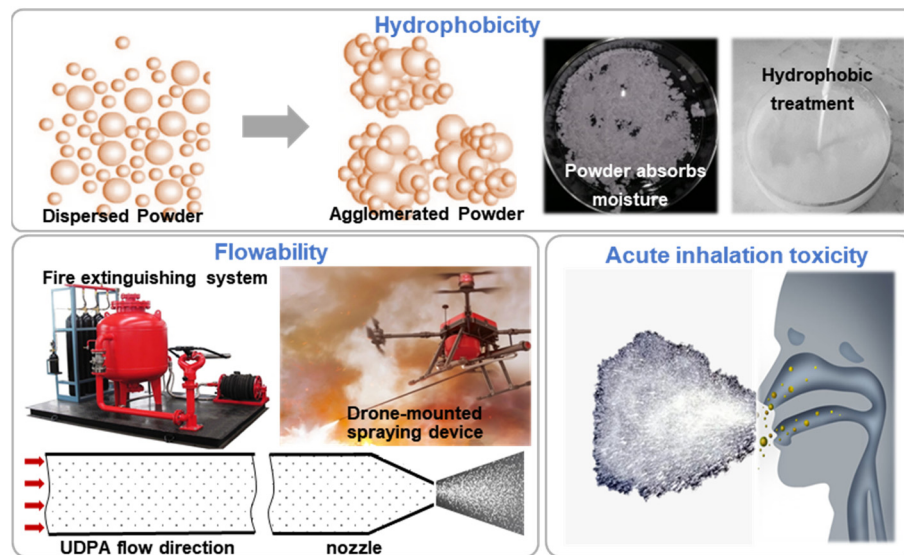


Figure 1. Demand for UDPA development.

In most instances, the UDPA is housed in a storage tank, with the particles transported through a nozzle using a propellant gas to act in fire environments. The flow properties of the extinguishing agent's particles exert a significant influence on these two processes [21]. Inadequate flowability may lead to the erosion of pipe walls during the transportation process, the clogging of nozzles, pipes, and valves, and ultimately impairing the extinguishing agent's spraying performance. Owing to the diminished kinetic energy of the spray, the settling rate of the extinguishing agent's particles is accelerated, preventing uniform and effective dispersal onto the surface of the burning material and diminishing the overall firefighting efficiency [22]. The preparation of ultrafine dry powder fire extinguishing agents with superior flowability has thus emerged as a prominent concern.

In order to develop free-flowing UDPAs, hydrophobic treatment, such as the addition of hydrophobic fumed silica, is first required [23]. Capillary bridges can form between particles in wet UDPAs. The hydrophobic coating prevents the formation of capillary bridges and thus prevents the agglomeration of UDPAs [24,25]. Often, functional additives help to reduce the forces between the particles, i.e., van der Waals, electrostatic, and capillary forces. Hydrophobic additives improve the flow of UDPAs by reducing the friction on the particle surface. Other additives such as metal stearates, perlite, and active white clay, which are common additives in fire extinguishing agents, can also improve the flow characteristics of UDPAs [23]. Optimizing the content of functional additives in UDPAs is rather challenging. When the proportion of additives is too low, the operational properties of the powder deteriorate and the guaranteed shelf life is shortened. The flow of the composition becomes increasingly poor if functional additives are added much in comparison to the surface area of the powder particles because of the friction and increased contact between them.

The aim of this study is to investigate the optimum amount of different functional additives to be added in UDPAs to enhance their flowability and improve their fire extin-

guishing efficiency. Furthermore, despite the primary application of ultrafine dry powder extinguishing agents for fire protection in unoccupied environments, their deployment may inevitably result in human inhalation upon release.

2. Materials and Experimental Section

2.1. Materials

All reagents were used as received from chemical reagent companies without any further purification. ADP was used as the main component of the UDPA with a purity greater than 99%, purchased from Shandong Dingxin Biotechnology Co., Ltd., Weifang, China. Fumed silica was purchased from Shanghai Aladdin Biochemical Technology Co. Ltd. (hydrophobic-120 type), 99.8% metal-based, with a particle size of 7–40 nm and specific surface area of $120 \text{ m}^2/\text{g}$. Perlite, magnesium stearate, and bentonite were selected and used as functional additives to further promote flow in ADP powders, and the optimum ratio for addition was investigated [23]. Perlite was purchased from Lingshou County Woyuan Mineral Products Processing Plant, $D_{100} \leq 74 \mu\text{m}$. Bentonite was also purchased from the company, $D_{100} \leq 10 \mu\text{m}$. Magnesium stearate was purchased from Myriad Chemical Reagents Ltd. with a MgO content of 6.7–7.5%.

2.2. Preparation of Samples

Figure 2 shows the preparation process and tests of the sample in this paper. The original ADP powder needed to be refined by an air jet mill firstly, purchased from Hosokawa Micron Powder Co., Ltd., Shanghai, China. The D_{90} of the refined ADP powders was about $5.408 \mu\text{m}$, shown in Figure 3. To address the moisture absorption properties of the refined ADP powder, fumed silica with hydrophobic properties was added to the ADP powder as a functional additive. The hydrophobic fumed silica both prevents agglomeration and is able to act as a flow-promoting functional additive. The optimal addition ratio of hydrophobic fumed silica was investigated, which was considered by both hydrophobicity and the Carr flow index. The fumed silica and ADP were mixed at different mass ratios and stirred in a water bath temperature of 80°C for 10 min. Fumed silica would be attached to the ADP surface during the process after these two kinds of powders were sufficiently dispersed. The mixed powders were then cooled down to room temperature and cured in a dryer for 15 min. Then, the powder samples were obtained and tested for hydrophobicity and flowability.

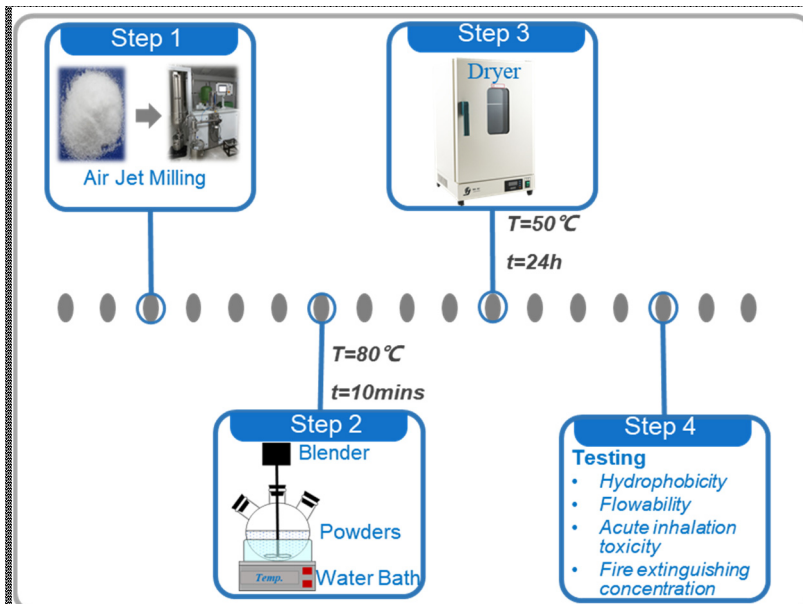


Figure 2. The preparation and tests for the UDPAs.

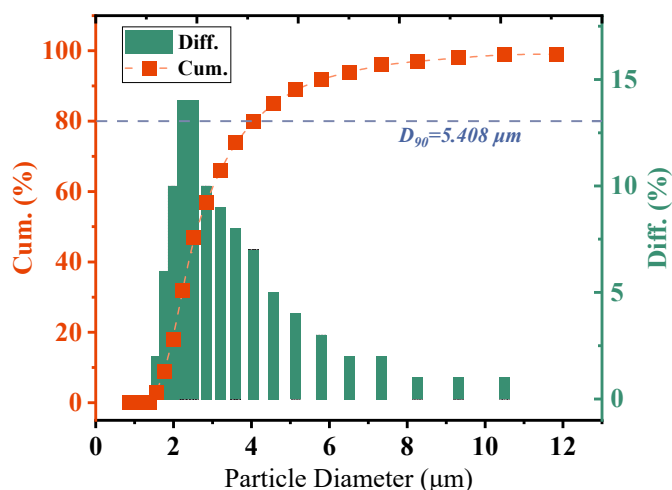


Figure 3. The particle diameter distribution of refined ADP.

The other three functional additives (i.e., perlite, bentonite, and magnesium stearate) are only able to act as flow-promoting functional additives. To determine the optimum proportion of the other three functional additives, ADP was first mixed with different proportions of the functional additives and stirred at 80 °C for 5 min. The optimum proportion of fumed silica was then added to the mixture and stirred for 10 min at the same conditions. Then, flowability was tested to determine the optimum ratio of the functional additives. The flowability of the samples with the other three functional additives added was then examined afterward. After screening, the UDPA with the best flowability could finally be designed.

2.3. Fire Suppression Test and Acute Inhalation Test

The fire suppression and acute inhalation studies were conducted within a 1 m³ cube space, shown in Figure 4a. An aerosol generator utilized dry air to create a finely dispersed UDPA-containing stream, which was introduced into the experimental area through the injection port (Figure 4b). Within this setting, three oil pans were arranged, each partially filled with petrol. The larger pan, with a diameter of 100 mm and a depth of 50 mm, was positioned in the center of the experimental space, while the two smaller pans, each with a diameter of 60 mm and a depth of 30 mm, were situated diagonally at the maximum distance from the injection port and 100 mm away from each surface. To confirm the minimum extinguishing concentration of the UDPA, a balance was employed to measure the powder consumption both before and after the flame was extinguished. Furthermore, a gas analyzer was deployed to detect variations in oxygen and CO levels within the space, ensuring that the extinction of the flame was not due to oxygen deprivation.

In order to verify whether the accidental inhalation of the UDPA will have any effect on human beings, a 60 s acute inhalation test was conducted using mice. Any abnormalities in the escape ability of the mice after acute inhalation and continuous feeding for three days were recorded to demonstrate the safety of the human body after the brief inhalation of the UDPA. In the acute inhalation test, four SPF-grade KM mice, with an equal distribution of male and female individuals (the females were not pregnant or lactating), weighing between 18 and 22 g, and bearing the qualification number No. 370726230100501763, were utilized. The mice were obtained from Jinan Ponyue Experimental Animal Breeding Co. As depicted in Figure 4c, four mice (both male and female) were placed in separate cages positioned at the four corners of the experimental chamber, at a height of 100 mm from the floor and a distance of 50 mm from the adjoining walls. Approximately 120 g of the UDPA was introduced into the chamber, and a 60 s observation period ensued after the completion of the spray to monitor any abnormal behavior in the mice.

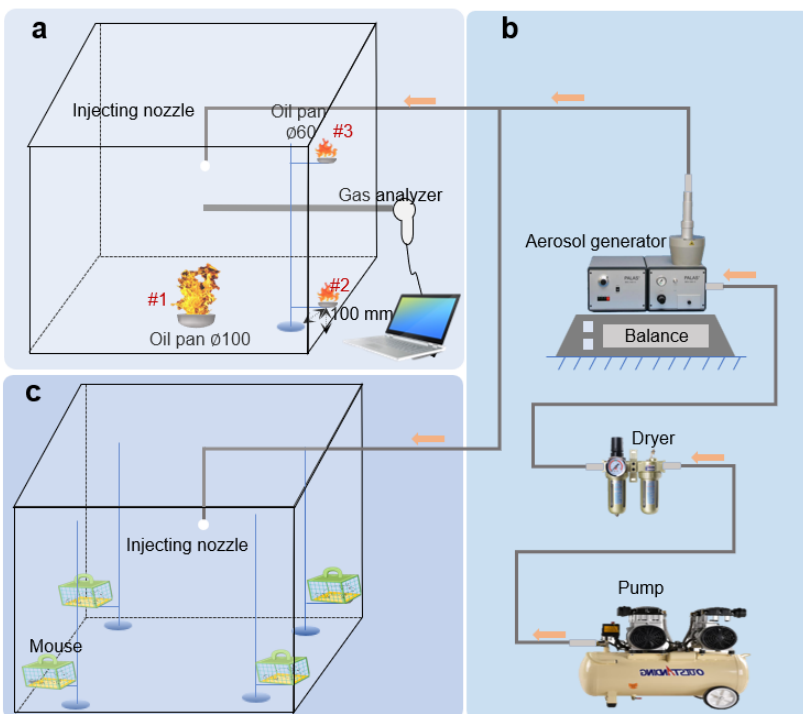


Figure 4. (a) Schematic diagram of 1 m^3 total flooding fire extinguishing experiment; (b) schematic diagram of aerosol generator system; (c) schematic diagram of acute inhalation toxicity experiments.

2.4. Characterizations

The particle size distribution was measured using SALD-2300 of Shimadzu Corporation of Japan. Hydrophobicity is mainly characterized by measuring the contact angle between the powder and the water droplet. The contact angle is an important parameter for characterizing the wettability of a material's surface and is the angle between the solid–liquid interface and the gas–liquid interface [24,26]. The contact angle tester, model SL200KB, was purchased from KINO Scientific Instrument Inc., Boston, MA, USA.

A wide range of parameters affect flowability, including the angle of repose, angle of collapse, angle of flatness, compressibility, and Carr flow index. In order for powder products to be comminuted, loaded, and conveyed, these parameters are critical [27,28]. The flowability of solid powders was measured by the powder comprehensive characteristic tester (BT-1001, Dandong Baxter Co., Ltd., Dandong, China). During the flowability testing process, the comprehensive powder testing instrument will first measure the angle of repose, compressibility, flat angle, uniformity, tap density, apparent density, and other indices during the flowability testing process. Then, the Carr flow index is obtained by summing the corresponding weightings according to the index weights table.

3. Results and Discussion

3.1. The Determination of the Optimum Amount of Hydrophobic Fumed Silica

The inclusion of hydrophobic fumed silica serves a dual purpose in the context of our study. Firstly, it prevents the agglomeration of finer ADP particles, thereby ensuring the uniform dispersion of ADP throughout the fire extinguishing agent. Additionally, it enhances the flowability of ADP, facilitating its effective deployment. However, it is worth mentioning that the impact of fumed silica additions on the UDPA requirements for flame extinction was found to be negligible, as reported by Hamins et al. [29]. Similarly, Rosser et al. [30] observed that fumed silica did not exhibit sufficient inhibitory properties towards hydrocarbon combustion.

In our investigation, the extinguishing agent samples primarily rely on ADP as the active ingredient responsible for fire suppression. Consequently, the inclusion of fumed silica leads to a reduction in the mass fraction of ADP, as the amount of fumed silica increases. However, it is advisable to incorporate a small quantity of fumed silica, provided

that the extinguishing agent satisfies the hydrophobic criteria. In our experimental setup, we prepared samples containing varying proportions of hydrophobic fumed silica (ranging from 2.0 to 10.0 wt.%), as detailed in Table 1.

Table 1. The mass fraction of fumed silica for different samples.

Samples	Mass Fraction (%)	
	ADP	Fumed Silica
S1	98.00	2.00
S2	96.00	4.00
S3	94.00	6.00
S4	92.00	8.00
S5	90.00	10.00

The microscopic morphology images of various samples are presented in Figure 5a. The pulverized ADP particles are about 2–5 microns in size and exhibit an ellipsoidal shape with a smooth surface and no attachment. The fine ADP has a large specific surface energy, and the particles agglomerate under the action of electrostatic and van der Waals forces [31]. The attached fine fumed silica particles in Samples S1–S5 are distinctly visible, giving rise to a ‘core-shell’ configuration. In order to ascertain the fumed silica content in the different samples, an XPS analysis was conducted, as depicted in Figure 5b,c, owing to the varying incorporations of hydrophobic fumed silica among the samples. ADP serves as the primary substrate for powder preparation, thereby resulting in the manifestation of peaks corresponding to P 2p, C 1s, N 1s, and O 1s in all the samples. The pronounced characteristic of the powder samples impregnated with hydrophobic fumed silica is the presence of the Si element as an augmentation to the pure ADP powder. Notably, in comparison to the pure ADP powder, the other samples exhibit an additional peak (Si 2p) at 101.98 eV [32]. The Si elemental content on the particle surface in Samples S1–S5 escalates from 15% to 27% with the inclusion of hydrophobic fumed silica. The discrepancy in the Si elemental content between the samples lucidly demonstrates the variability in the quantities of hydrophobic fumed silica adhesions on their surfaces.

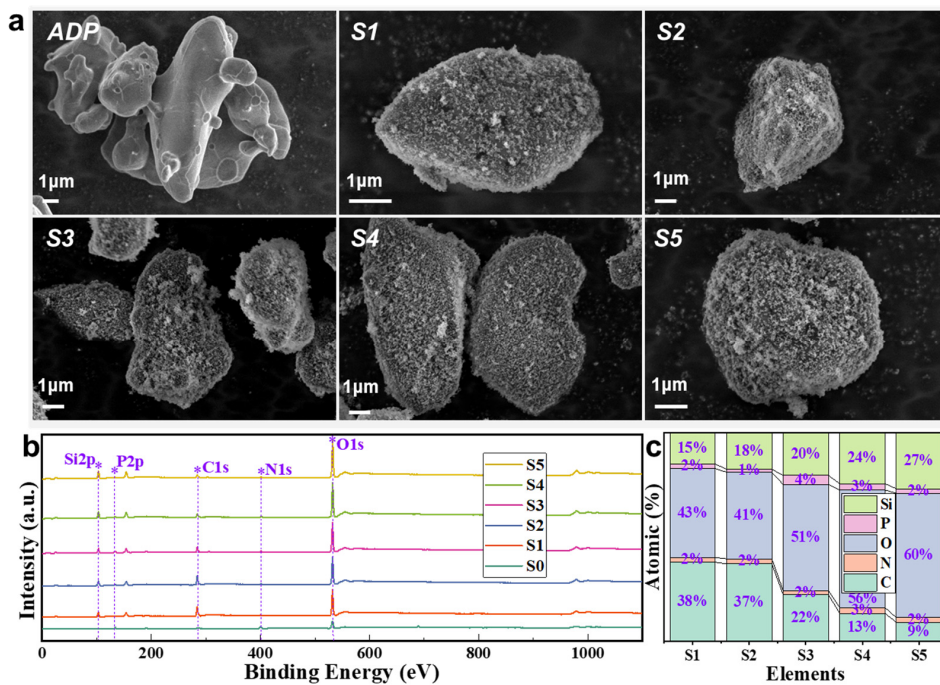


Figure 5. (a) SEM image of different samples; (b) XPS characterizations of different samples; (c) surface element distribution of different samples.

Firstly, we determined the water contact angle of the different samples. In Figure 6, the water contact angle increases from 113.45° to 129.63° with an increase in fumed silica's mass fraction from 2% to 6%. The hydrophobicity of the extinguishing agent doesn't change much as the mass fraction of fumed silica increases from 6% to 10%. It can be obtained that the hydrophobicity of the UDPA reaches a good state when the mass fraction of fumed silica is above 6%.

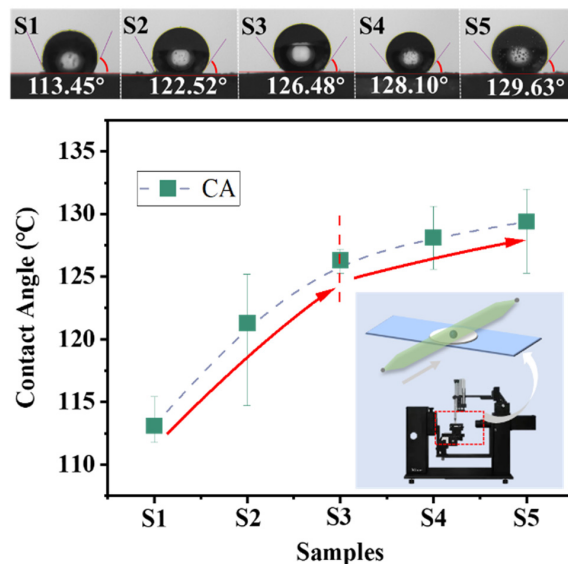


Figure 6. The contact angles of different samples.

Next, the flowability of the above five samples were studied. There is no clear definition of powder flowability and no uniform evaluation method. The common evaluation method is basically to test a single physical property of powders, such as the angle of repose, plate angle, compressibility, etc., to evaluate the flowability of powders based on the performance [33]. Many testing methods exist, but not every method is suitable for UDPAs, so it is necessary to compare and select the evaluation method that is most suitable. The Carr flow index method is a more comprehensive method for evaluating powder flowability [34]. Each performance test result is assigned an index with a maximum value of 25 based on a measurement of four sub-indices, which are the repose angle, compressibility, plate angle, and uniformity. The angle of repose refers to the angle formed by the free surface of the powder accumulation layer in static equilibrium with the horizontal plane. The smaller the angle of repose, the better the flowability of the powders. The ratio of the difference between the vibrational density and the bulk density of the sample to the vibrational density is the compressibility. The smaller the degree of compression, the better the flowability of the powder. The flat plate angle refers to the average of the angle between the free surface of the powders on the plate and the plate and the angle after being vibrated. The smaller the plate angle, the more mobile the powder. Uniformity is the ratio of particle diameter D_{60} to D_{10} and can be used to determine the size of mutual agglutination. In order to evaluate the flowability of the powder in a comprehensive way, the total value is obtained by adding points as the Carr flow index. The higher the value, the better the powder's flowability.

Table 2 gives the measured data for the angle of repose, compression, flatness angle, and homogeneity of the five samples, as well as the Carr flow index obtained. It can be directly obtained from Figure 7 that the S3 and S4 samples have the highest Carr flow index and the best flowability of the powder, i.e., the best flowability of the extinguishing agent with a 6% and 8% mass fraction of fumed silica added. In combination with the water contact angle, the amount of fumed silica added should be as small as possible to ensure hydrophobicity, and the optimum amount of fumed silica added was finally determined to be 6 wt.%. When the level of fumed silica additive is insufficient to fully cover the surface of ADP particles, the ability of fumed silica particles to act as separators for the ADP particles is compromised. This, in turn,

allows for the interaction force between ADP particles to continue being chiefly determined by direct contact, thereby impeding enhancements in the flowability of the extinguishing agent powder. Both Anthony [35] and Shinohara [36] have demonstrated that particles with irregular shapes have a propensity to interlock, consequently leading to increased internal friction.

Table 2. Flow and fluidization behaviors of samples with fumed silica added.

Samples	Angle of Repose (°)	Angle of Collapse (°)	Compressibility (%)	Angle of Plate (°)	Degree of Dispersion	Uniformity	Carr Flow Index
S1	37.38	13.16	34.07	65.78	59.80	2.87	60.00
S2	42.76	11.39	34.21	60.01	63.50	2.83	60.50
S3	38.12	10.90	33.60	50.85	52.70	2.95	64.00
S4	37.27	13.26	32.33	49.18	43.70	2.86	64.00
S5	40.58	13.41	35.73	56.81	37.40	2.93	62.00

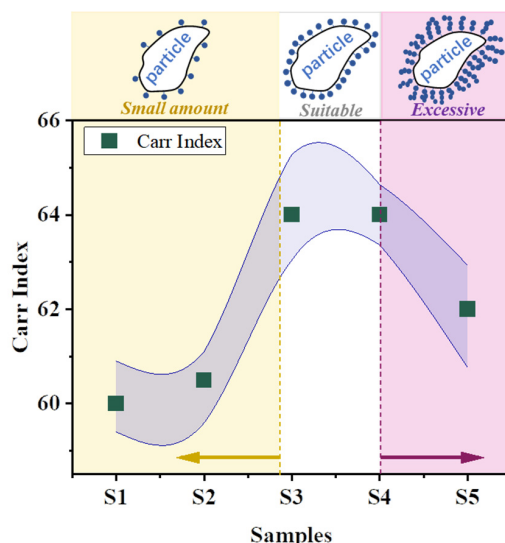


Figure 7. The Carr flow indexes of different samples with fumed silica added.

Lattice spacing within the ADP particles is expanded when uniformly adhered with appropriate fumed silica additives, resulting in a reduced interaction force between the particles [27,37]. Additionally, the hydrophobic fumed silica particles adhere to the surface of ADP particles create an effect akin to having a ‘thin film’ covering the particles, thereby performing the function of a ‘lubricant’. This ‘lubricant’ ultimately diminishes the mutual friction occurring on the surface of ADP particles, thus effecting an improvement in the fluidity of the powder fire extinguishing agent.

The excessive addition of fumed silica leads to surplus silica particles being trapped in the interstices between the ADP particles. These excess fumed silica particles form branched chains and bridges among the ADP particles, impeding the relative movement of ADP particles. Thus, inter-particle flow hindrance results since the ADP particles become tightly interconnected through chains or bridges that are challenging to disengage, thus impairing flowability. Consequently, the optimal flow properties of the powder are observed when a 6% mass fraction of fumed silica is added, thereby reducing inter-particle cohesion and dynamic flow resistance.

3.2. Determination of Optimum Amount of Three Functional Additives to Promote Flowability of UDPA

Based on the determination of 6% hydrophobic fumed silica as the most suitable addition, perlite, magnesium stearate, and bentonite were proposed to be further added as functional additives to improve the flowability of the UDPA. The mass fraction of functional

additives in different samples is presented in Table 3. The P, M, and B in the samples stand for perlite, magnesium stearate, and bentonite, respectively.

Table 3. Mass fraction of components of powder samples.

Samples	Mass Fraction (%)				
	ADP	Fumed Silica	Bentonite	Magnesium Stearate	Perlite
B1	93.50	6.00	0.50	/	/
B2	93.00	6.00	1.00	/	/
B3	92.50	6.00	1.50	/	/
B4	92.00	6.00	2.00	/	/
M1	93.50	6.00	/	0.50	/
M2	93.00	6.00	/	1.00	/
M3	92.50	6.00	/	1.50	/
M4	92.00	6.00	/	2.00	/
P1	93.50	6.00	/	/	0.50
P2	93.25	6.00	/	/	0.75
P3	93.00	6.00	/	/	1.00
P4	92.00	6.00	/	/	2.00

As shown in Figure 8a, the deduced Carr flow index varies with the different mass fraction of perlite added. Table 4 shows the different indexes to characterize the flowability of powder samples. In the case of a single index, the value is not monotonically increasing or decreasing. The P3 sample, which has 6 wt.% fumed silica and 1.0 wt.% perlite added, has the highest Carr flow index and the best flowability. However, the Carr flow index of the P3 sample is lower than that of the S3 sample.

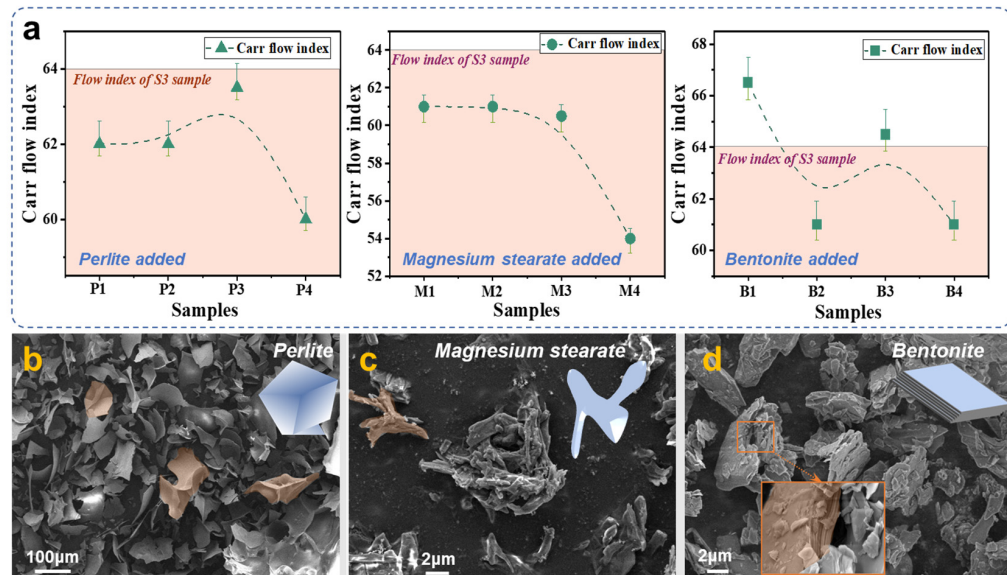


Figure 8. (a) The Carr flow indexes of different samples with perlite, magnesium stearate, and bentonite added; (b) the SEM image of perlite; (c) the SEM image of magnesium stearate; (d) the SEM image of bentonite.

For the samples with magnesium stearate added, as the mass fraction of magnesium stearate increases, the repose angle increases and the plate angle decreases, shown in Table 5. The regularity of the compressibility and uniformity was not obvious, but extreme points

were observed in all M4 samples. Powder samples became less flowable as magnesium stearate was added, resulting in a decreasing Carr flow index. It is also found that the Carr flow index of the M1 to M4 samples is lower than that of S3, which indicates that the addition of magnesium stearate reduced the flowability of the powder samples instead. The results suggest that magnesium stearate may not be suitable as a functional additive to promote the flowability of ADP powder.

Table 4. Flow and fluidization behaviors of samples with perlite added.

Samples	Angle of Repose (°)	Angle of Collapse (°)	Compressibility (%)	Angle of Plate (°)	Degree of Dispersion	Uniformity	Carr Flow Index
P1	43.21	9.39	32.07	55.50	35.90	3.57	62.00
P2	43.55	11.65	32.11	51.34	46.50	3.41	62.00
P3	39.41	14.21	32.56	54.81	41.60	3.34	63.50
P4	44.11	12.54	33.15	57.69	53.10	3.45	60.00

Table 6 shows the flow and fluidization behaviors of samples with bentonite added, including the indexes of the repose angle, compressibility, plate angle, and uniformity. The Carr flow index was deduced from the above indexes. Statistically, the compressibility trend is the closest to the Carr flow index trend, with B1 having the highest flowability and B3 having the second highest. The Carr flow index is shown to decrease overall as more bentonite is added, indicating that the flowability decreases. The B1 sample, which had 6 wt.% fumed silica and 0.5 wt.% bentonite added, has the highest Carr flow index and the best flowability. Comparing with the Carr flow index of the S3 sample, the B1 and B3 samples have higher indexes than that of the S3 sample. The result shows that the optimum mass fraction of bentonite added is 0.5%, while more might decrease the flowability of ADP powders.

Table 5. Flow and fluidization behaviors of samples with magnesium stearate added.

Samples	Angle of Repose (°)	Angle of Collapse (°)	Compressibility (%)	Angle of Plate (°)	Degree of Dispersion	Uniformity	Carr Flow Index
M1	41.20	12.61	33.60	58.04	52.80	3.31	61.00
M2	43.48	13.95	34.09	58.54	46.70	2.98	61.00
M3	43.08	12.32	31.96	61.48	37.80	2.85	60.50
M4	47.16	12.90	35.72	63.62	58.40	2.99	54.00

Table 6. Flow and fluidization behaviors of samples with bentonite added.

Samples	Angle of Repose (°)	Angle of Collapse (°)	Compressibility (%)	Angle of Plate (°)	Degree of Dispersion	Uniformity	Carr Flow Index
B1	41.64	11.73	30.64	44.29	61.40	2.66	66.50
B2	41.62	11.64	32.66	56.70	42.80	2.74	61.00
B3	41.29	10.70	31.35	55.79	44.60	2.75	64.50
B4	44.30	11.06	32.88	48.69	46.20	2.70	61.00

Figure 8b–d illustrate the micro-morphological traits of the three functional additives—perlite, magnesium stearate, and bentonite. Perlite, in its original state, exhibits a porous nature and assumes a fragmented form with rhombic angles upon comminution. The introduction of such a structural functional additive curtails the slippage of ADP particles against each other, thereby mitigating the flowability of ADP powder. Magnesium stearate particles are minute, approximately 2 μm , and tend to agglomerate, indicating pronounced

van der Waals forces and inter-particle cohesion. This phenomenon possibly accounts for the absence of flow-promoting characteristics upon its integration into ADP powders. Conversely, bentonite, with a particle size of roughly $5\text{ }\mu\text{m}$, demonstrates a more dispersed and notably flaky structure. Coupled with the assessment of the Carr flow index measurement results, it becomes apparent that additives characterized by a flaky structure circumvent the compromised flowability arising from the irregular shape of the ADP particles. Nevertheless, there lies a threshold for the quantity of functional additives, as an excessive amount may exert detrimental effects on flowability owing to increased friction. Therefore, the incorporation of 0.5 wt.% bentonite into ADP allows for the observation of an optimal flow effect.

3.3. The Experiments of Fire Extinguishing and Acute Inhalation Toxicity

Sample B1 exhibited superior flowability in all the samples and was utilized for fire suppression as well as acute inhalation investigations. As shown in Figure 9a, during one of the fire suppression experiments, the gas analyzer recorded data reflecting an increase in smoke temperature and CO content at the onset of the experiment, concurrently with a decrease in oxygen content due to the sustained combustion of the flame. Throughout the three fire extinguishing experiments, the lowest observed oxygen content was 17.2%, 18.0%, and 18.3%, which exceeded the self-extinguishing oxygen content threshold of 14%. When the UDPA was released, there was a marked rise in CO content as the flame combustion was suppressed. The carrier gas stream for the UDPA was air, leading to a gradual increase in oxygen content. Approximately 60 s after the deployment of the UDPA, the flame was fully extinguished. Across the three fire extinguishing experiments (Figure 9b was given as the sample), it was noted that flame #3 was extinguished first, followed by flames #1 and #2 in sequence. The observed phenomenon may be attributed to the flow of gas within the experimental chamber. Under the influence of the primary flame, the heated air rose upwards, formed swirling patterns, and entrained around the periphery of the flame, leading to a higher concentration at the #3 position. Upon the continuous injection of the UDPA, the concentration at positions #1 and #2 gradually increased to the extinguishing levels and subsequently ceased. The amount of powder consumed during the three fire extinguishing experiments was 38.0 g, 42.2 g, and 44.4 g, with an average minimum extinguishing concentration of 41.5 g/m^3 , which was better than the reported values of 79.8 g/m^3 and $60\text{--}160\text{ g/m}^3$ [38,39].

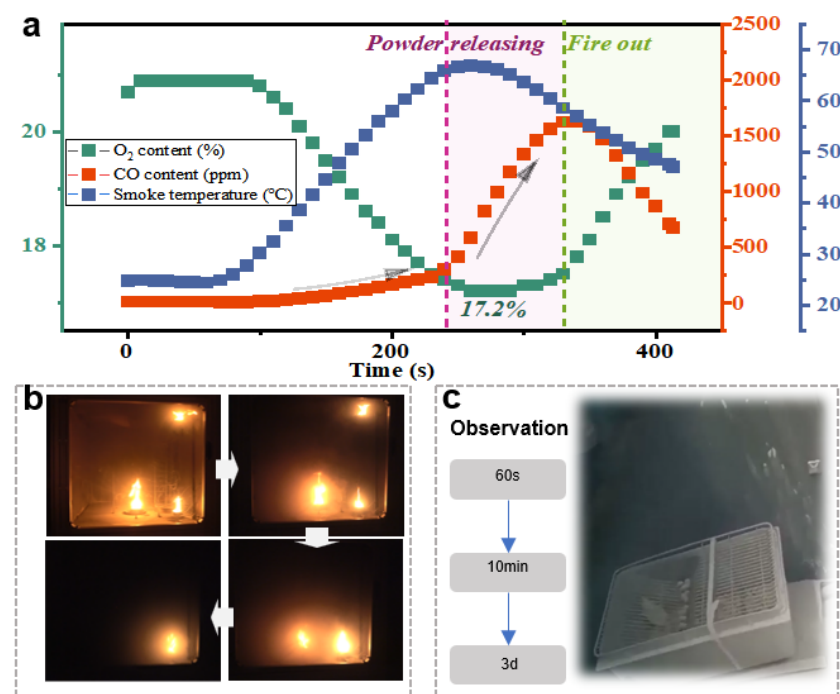


Figure 9. (a) The gas analysis and (b) fire phenomenon in a fire extinguishing experiment; (c) experimental procedure for acute inhalation toxicity in mice.

Showed in Figure 9c, in the acute inhalation experiment, the mice were removed from their cages 10 min after 120 g of the UDPA had been introduced into the chamber and found to be in good condition, with no fatalities and normal escape abilities. With sustained care and observation over the next three days, all four mice remained alive and exhibited either stable or slightly increased body weights. These results attest to the absence of the acute inhalation toxicity of the UDPA.

4. Conclusions

In this study, our aim was to enhance the flow characteristics of the UDPA while preserving its hydrophobic and fire extinguishing properties. We investigated the impact of incorporating hydrophobic fumed silica on the hydrophobicity and flow properties of the UDPA and the effects of adding bentonite, magnesium stearate, and perlite on improving its flowability. Furthermore, experiments were carried out to assess the fire extinguishing concentration and acute inhalation toxicity of the modified UDPA. Our key findings can be succinctly summarized as follows:

1. The contact angle with water droplets increases with the mass fraction of fumed silica. The hydrophobicity of the UDPA reaches a good state when the mass fraction of fumed silica is above 6%, since the contact angle with water droplets of the S3 sample is 126.48°.
2. The S3 sample has the highest Carr flow index and the best flowability, i.e., the best flowability of the extinguishing agent with a 6% mass fraction of fumed silica added. Small amounts of fumed silica additions do not provide adequate lubrication, and excessive additions result in excess fumed silica particles being trapped in the gaps between ADP particles increasing friction.
3. The flowability of the ADP powders is improved by adding small amounts of bentonite (0.5 wt.%). Magnesium stearate and perlite even reduce the flowability of ADP powders. The minimum fire extinguishing concentration of the designed UDPA was 41.5 g/m³, better than the values reported in the literature.
4. There is no acute inhalation toxicity associated with the designed UDPA. This was verified by monitoring the condition of the mice exposed to nearly three times the fire extinguishing concentration for durations of 60 s and 10 min. Following exposure, the mice were removed, nourished, and observed for 3 days, revealing no adverse effects.

Author Contributions: Conceptualization, G.L. and J.Z.; methodology, J.Z.; validation, Y.F., S.L. and H.Z.; formal analysis, G.L. and J.Z.; investigation, G.L. and Y.Z.; resources, J.Z. and H.Z.; data curation, G.L. and J.Z.; writing—original draft preparation, G.L. and J.Z.; writing—review and editing, G.L., J.Z. and H.Z.; supervision, J.Z. and H.Z.; funding acquisition, J.Z. and H.Z. All authors have read and agreed to the published version of the manuscript.

Funding: This research was supported by the National Natural Science Foundation of China (No. 52304264), China Postdoctoral Science Foundation (2022M723016) and Fundamental Research Funds for the Central Universities (No. WK2320000064). Also, it was supported by Tianjin Key Laboratory of Fire Safety Technology the under Grant No. 2023TKLFST02.

Institutional Review Board Statement: Not applicable.

Informed Consent Statement: Not applicable.

Data Availability Statement: Data are contained within the article.

Conflicts of Interest: The authors declare no conflicts of interest.

References

1. Molina, M.J.; Rowland, F.S. CFCs in the environment. *Nature* **1974**, *8*.
2. Zhao, J.; Lu, S.; Fu, Y.; Shahid, M.U.; Zhang, H. Application of ultra-fine dry chemicals modified by POTS/OBS for suppressing aviation kerosene pool fire. *Fire Saf. J.* **2020**, *118*, 103148. [[CrossRef](#)]
3. Zhao, J.; Fu, Y.; Yin, Z.; Xing, H.; Lu, S.; Zhang, H. Preparation of hydrophobic and oleophobic fine sodium bicarbonate by gel-sol-gel method and enhanced fire extinguishing performance. *Mater. Des.* **2020**, *186*, 108331. [[CrossRef](#)]

4. Trees, D.; Seshadri, K. Experimental studies of flame extinction by sodium bicarbonate (NaHCO_3) powder. *Combust. Sci. Technol.* **2007**, *122*, 215–230. [[CrossRef](#)]
5. Jiang, H.; Bi, M.; Li, B.; Ma, D.; Gao, W. Flame inhibition of aluminum dust explosion by NaHCO_3 and $\text{NH}_4\text{H}_2\text{PO}_4$. *Combust. Flame* **2019**, *200*, 97–114. [[CrossRef](#)]
6. Payri, R.; Gimeno, J.; Martí-Aldaraví, P.; Carvallo, C. Parametrical study of the dispersion of an alternative fire suppression agent through a real-size extinguisher system nozzle under realistic aircraft cargo cabin conditions. *Process Saf. Environ. Prot.* **2020**, *141*, 110–122. [[CrossRef](#)]
7. Ewing, C.T.; Hughes, J.T.; Carhart, H.W. The extinction of hydrocarbon flames based on the heat-absorption processes which occur in them. *Fire Mater.* **1984**, *8*, 148–156. [[CrossRef](#)]
8. Ewing, C.T.; Faith, F.R.; Romans, J.B.; Hughes, J.T.; Carhart, H.W. Flame extinguishment properties of dry chemicals: Extinction weights for small diffusion pan fires and additional evidence for flame extinguishment by thermal mechanisms. *J. Fire Prot. Eng.* **1992**, *4*, 35–51. [[CrossRef](#)]
9. Zhao, J.; Yin, Z.; Shahid, M.U.; Xing, H.; Cheng, X.; Fu, Y.; Lu, S. Superhydrophobic and oleophobic ultra-fine dry chemical agent with higher chemical activity and longer fire-protection. *J. Hazard. Mater.* **2019**, *380*, 120625. [[CrossRef](#)]
10. Zhao, J.; Xue, F.; Fu, Y.; Cheng, Y.; Yang, H.; Lu, S. A comparative study on the thermal runaway inhibition of 18,650 lithium-ion batteries by different fire extinguishing agents. *iScience* **2021**, *24*, 102854. [[CrossRef](#)]
11. Laryea, A.E.N.; Wanxing, R.; Qing, G.; Zenghui, K. Spontaneous Coal Combustion, Direct and Indirect Impact on Mining in China: A Prospective Review and Proposal of a Five-Level Comprehensive Mine Safety Management Structure (5L-CMSMS) Coupled with Hazard Zoning and Barrier Systems. *Combust. Sci. Technol.* **2024**, *1*–33. [[CrossRef](#)]
12. Cheng, C.; Si, R.; Wang, L.; Jia, Q.; Xin, C. Explosion and explosion suppression of gas/deposited coal dust in a realistic environment. *Fuel* **2024**, *357*, 129710. [[CrossRef](#)]
13. Jin, K.-Y.; Wang, Y.-H.; Zhou, X.-H.; Deng, R.; Hu, C.; Wen, H. Behavior of super-sized thin-walled CFDST columns for wind turbine towers subjected to combined loads: Experiment. *Eng. Struct.* **2024**, *303*, 117458. [[CrossRef](#)]
14. You, F.; Shaik, S.; Rokonuzzaman, M.; Rahman, K.S.; Tan, W.-S. Fire risk assessments and fire protection measures for wind turbines: A review. *Heliyon* **2023**, *9*, e19664. [[CrossRef](#)] [[PubMed](#)]
15. Ilah, N.; Alshbatat, A. Fire Extinguishing System for High-Rise Buildings and Rugged Mountainous Terrains Utilizing Quadrotor Unmanned Aerial Vehicle. *Int. J. Image Graph. Signal Process.* **2018**, *10*, 23–29. [[CrossRef](#)]
16. Wang, K.; Yuan, Y.; Chen, M.; Lou, Z.; Zhu, Z.; Li, R. A Study of Fire Drone Extinguishing System in High-Rise Buildings. *Fire* **2022**, *5*, 75. [[CrossRef](#)]
17. Yan, C.; Pan, X.; Hua, M.; Li, S.; Guo, X.; Zhang, C. Study on the fire extinguishing efficiency and mechanism of composite superfine dry powder containing ferrocene. *Fire Saf. J.* **2022**, *130*, 103606. [[CrossRef](#)]
18. Li, H.; Feng, L.; Du, D.; Guo, X.; Hua, M.; Pan, X. Fire suppression performance of a new type of composite superfine dry powder. *Fire Mater.* **2019**, *43*, 905–916. [[CrossRef](#)]
19. Rouhana, L.L.; Jaber, J.A.; Schlenoff, J.B. Aggregation-resistant water-soluble gold nanoparticles. *Langmuir* **2007**, *23*, 12799–12801. [[CrossRef](#)]
20. Gregory, J. Monitoring particle aggregation processes. *Adv. Colloid Interface Sci.* **2009**, *147*, 109–123. [[CrossRef](#)]
21. Krantz, M.; Zhang, H.; Zhu, J. Characterization of powder flow: Static and dynamic testing. *Powder Technol.* **2009**, *194*, 239–245. [[CrossRef](#)]
22. Li, H.; Du, D.; Guo, X.; Hua, M.; Pan, X. Experimental Study on the Optimum Concentration of Ferrocene in Composite Ultrafine Dry Powder. *Fire Technol.* **2019**, *56*, 913–936. [[CrossRef](#)]
23. Shamsutdinov, A.S.; Kondrashova, N.B.; Valtsifer, I.V.; Bormashenko, E.; Huo, Y.; Saenko, E.V.; Pyankova, A.V.; Valtsifer, V.A. Manufacturing, properties, and application of nanosized superhydrophobic spherical silicon dioxide particles as a functional additive to fire extinguishing powders. *Ind. Eng. Chem. Res.* **2021**, *60*, 11905–11914. [[CrossRef](#)]
24. Afrassibian, Z.; Leturia, M.; Benali, M.; Guessasma, M.; Saleh, K. An overview of the role of capillary condensation in wet caking of powders. *Chem. Eng. Res. Des.* **2016**, *110*, 245–254. [[CrossRef](#)]
25. Drmann, M.; Schmid, H.J. Simulation of Capillary Bridges between Particles. *Procedia Eng.* **2015**, *102*, 14–23. [[CrossRef](#)]
26. Lin, Z.; Liu, W.; Tan, J. Properties of (meth)acrylate copolymer grafted with long fluorinated side chain prepared by “graft onto” strategy. *J. Appl. Polym. Sci.* **2018**, *135*, 45894. [[CrossRef](#)]
27. Tomas, J.; Kleinschmidt, S. Improvement of flowability of fine cohesive powders by flow additives. *Chem. Eng. Technol.* **2009**, *32*, 1470–1483. [[CrossRef](#)]
28. Tan, G.; Morton, D.A.V.; Larson, I. On the methods to measure powder flow. *Curr. Pharm. Des.* **2015**, *21*, 5751–5765. [[CrossRef](#)] [[PubMed](#)]
29. Hamins, A. Flame extinction by sodium bicarbonate powder in a cup burner. *Symp. Combust.* **1998**, *27*, 2857–2864. [[CrossRef](#)]
30. Rosser Jr, W.; Inami, S.; Wise, H. The effect of metal salts on premixed hydrocarbon—Air flames. *Combust. Flame* **1963**, *7*, 107–119. [[CrossRef](#)]
31. Mahmoud, M.; Huitorel, B.; Fall, A. Rheology and agglomeration behavior of semi-crystalline polyamide powders for selective laser sintering: A comparative study of PA11 and PA12 formulations. *Powder Technol.* **2024**, *433*, 119279. [[CrossRef](#)]
32. Vanitha, N.; Jeyalakshmi, R. Structural study of the effect of nano additives on the thermal properties of metakaolin phosphate geopolymers by MASNMR, XPS and SEM analysis. *Inorg. Chem. Commun.* **2023**, *153*, 110758. [[CrossRef](#)]

33. Kaleem, M.A.; Alam, M.Z.; Khan, M.; Jaffery, S.H.I.; Rashid, B. An experimental investigation on accuracy of Hausner Ratio and Carr Index of powders in additive manufacturing processes. *Met. Powder Rep.* **2021**, *76*, S50–S54. [[CrossRef](#)]
34. Hao, T. Understanding empirical powder flowability criteria scaled by Hausner ratio or Carr index with the analogous viscosity concept. *RSC Adv.* **2015**, *5*, 57212–57215. [[CrossRef](#)]
35. Anthony, J.L.; Marone, C. Influence of particle characteristics on granular friction. *J. Geophys. Res. Solid Earth* **2005**, *110*, B08409. [[CrossRef](#)]
36. Shinohara, K.; Oida, M.; Golman, B. Effect of particle shape on angle of internal friction by triaxial compression test. *Powder Technol.* **2000**, *107*, 131–136. [[CrossRef](#)]
37. Yang, J.; Sliva, A.; Banerjee, A.; Dave, R.N.; Pfeffer, R. Dry particle coating for improving the flowability of cohesive powders. *Powder Technol.* **2005**, *158*, 21–33. [[CrossRef](#)]
38. Chen, T.; Fu, X.C.; Xia, J.J.; Jing, L.S.; Hu, C. Study on fire extinguishing performance of superfine powder fire extinguishing agent in a cup burner. In Proceedings of the 2015 International Conference on Power Electronics and Energy Engineering, Hong Kong, China, 19–20 April 2015.
39. Ewing, C.T.; Faith, F.R.; Hughes, J.T.; Carhart, H.W. Flame extinguishment properties of dry chemicals: Extinction concentrations for small diffusion pan fires. *Fire Technol.* **1989**, *25*, 134–149. [[CrossRef](#)]

Disclaimer/Publisher’s Note: The statements, opinions and data contained in all publications are solely those of the individual author(s) and contributor(s) and not of MDPI and/or the editor(s). MDPI and/or the editor(s) disclaim responsibility for any injury to people or property resulting from any ideas, methods, instructions or products referred to in the content.